Inelastic Scattering of Protons from ^{16}O and the Spin-Dependent Part of the Effective Interaction

Sam M. Austin and P. J. Locard*†
Department of Physics and Cyclotron Laboratory, Michigan State University, East Lansing, Michigan 48823

and

S. N. Bunker,‡ J. M. Cameron,§ J. Reginald Richardson, and J. W. Verba‖
Department of Physics, University of California, Los Angeles, California 90024

and

W. T. H. van Oers**
Department of Physics, University of Manitoba, Winnipeg, Canada
(Received 23 April 1970; revised manuscript received 18 January 1971)

Angular distributions for the $^{16}O(p,p')^{16}O$ reaction leading to the $J^\pi = 2^-$ state at 8.88 MeV and the doublet of states at 6.05 MeV (0^+) and 6.13 MeV (3^-) have been measured at 23.4, 24.5, 27.3, 30.1, 34.1, 36.8, 39.7, 43.1, and 46.1 MeV. In the distorted-wave approximation (DWA) with central forces, the transition to the unnatural-parity (2^-) state can occur only through the spin-dependent part $V_{10} = V_\sigma f(r)\vec{\sigma}_i \cdot \vec{\sigma}_p$ of the effective two-nucleon interaction. The experimental angular distributions were compared with DWA calculations assuming $f(r)$ has a Yukawa shape with a range of 1.0 F. Normalization to the measured cross sections determined the strength V_σ, which was found to decrease rapidly from a magnitude of 53 MeV to about 23 MeV between $E_p = 17.0$ MeV and $E_p = 30.1$ MeV, and then to decrease slowly to about 16 MeV at $E_p = 46.1$ MeV. The shape of the experimental angular distributions for the inelastic scattering to the 2^- state are well represented by the DWA at the lower energies, but the agreement deteriorates as the energy increases. The forward peak in the higher-energy data occurs at larger angles than the DWA prediction. The cross section calculated using a pseudopotential derived from the impulse approximation is too small by a factor of about 4 at all energies. The possible contribution of other reaction mechanisms to the cross section for scattering to the 2^- state is discussed. An analysis of the transition to the 6.1-MeV doublet is used to estimate the strength V_c of the spin-isospin-independent part V_{00} of the effective two-nucleon interaction. The experimental angular distributions for the 6.1-MeV doublet were also compared with the predictions of the impulse approximation.

I. INTRODUCTION

The spin-dependent parts of the effective two-nucleon interaction can contribute to an inelastic proton scattering cross section whenever spin angular momentum $S = 1$ is transferred to the target nucleus. In terms of the transferred spin, isospin, orbital angular momentum, and total angular momentum, $\vec{S}$, $\vec{T}$, $\vec{L}$, and $\vec{J}$, the selection rules for inelastic nucleon scattering in the local distorted-wave approximation (DWA) are[1]

$$\begin{aligned} &\vec{J} = \vec{J}_f - \vec{J}_i, \\ &\vec{S} = \vec{J} - \vec{L}, \qquad S = 0, 1, \\ &\vec{T} = \vec{T}_f - \vec{T}_i, \quad T = 0, 1, \\ &\Delta\pi = (-1)^L, \end{aligned} \tag{1}$$

where $\Delta\pi$ denotes the change in parity. The symbols $\vec{J}_i$, $\vec{T}_i$ and $\vec{J}_f$, $\vec{T}_f$ denote the spin and isospin of the initial and final state, respectively. From these relations it is seen that $S = 1$ is allowed unless both the initial and final states have $J = 0$ and the same parity. Thus the spin-dependent part of the force contributes to most transitions and it must be understood before one can obtain accurate spectroscopic information from inelastic scattering.

Unfortunately, while $V_{ST} = V_{11}$ is fairly well known,[2-7] only a few values of $V_{ST} = V_{10}$ appear in the literature,[8-13] and these are at widely scattered energies. One can conclude only that V_{10} is fairly weak compared to the spin-isospin-independent component V_{00}.

The principal experimental measurements reported in this paper are angular distributions for inelastic proton scattering leading to the 2^-, $T = 0$ state at 8.88 MeV in ^{16}O at nine proton energies between 23.4 and 46.1 MeV. This transition is exceptionally favorable for studies of V_{10}, since in the DWA the relations of Eq. (1) allow only $S = 1$ and $T = 0$. Thus, for central forces, only V_{10} can contribute to the cross section. The differential cross sections for exciting the unresolved 6.05-

MeV (0^+)-6.13-MeV (3^-) doublet are also reported. A preliminary analysis of these results is presented assuming the contribution of the 0^+ state can be neglected. The cross section for this transition is dominated by V_{00}.

If one wishes to determine the effective force by fitting the cross-section data, the reaction studied should satisfy at least two criteria. First, since the cross section depends on both the effective force and the wave functions of the nuclear states involved, these wave functions must be reasonably well known before information about the effective force can be obtained. The second criterion is that the reaction mechanism must be well described by the chosen model (the DWA). The first condition is satisfied, since random-phase-approximation (RPA) wave functions[14] are available for the states in ^{16}O considered in this paper. Unfortunately, there is evidence that compound-nuclear[15] and possibly multiple-excitation[16] processes contribute to the cross section at the lower energies. Thus the DWA analysis performed here may be unreliable, particularly for incident proton energies (E_p) smaller than 30 MeV, but these results represent the most detailed information about the energy dependence of V_{10} available at present, and the calculations should serve as a basis for more sophisticated analyses.

The experimental procedure and results are presented in Sec. II, while the DWA analysis to obtain V_{00} and V_{10} is given in Sec. III. In Sec. IV the calculated differential cross sections and the values of V_{00} and V_{10} are compared with previous work and with the predictions of an impulse-approximation (IA) pseudopotential. Possible contributions of other reaction mechanisms are also discussed.

II. EXPERIMENT

A. Experimental Method

The experimental part of this study was performed using the external beam facilities of the University of California, Los Angeles, sector-focused cyclotron. A detailed description of the experimental procedure used to study the elastic and inelastic scattering of protons from oxygen has been given previously,[17] and only a brief summary is included here.

A 10.75-in.-diam cylindrical cell with a 2.0-in.-high gap extending over 330° contained the oxygen gas. For laboratory angles greater than 50° the scattered particles were detected by an array of four scintillation detectors. The counting geometry for each of the detectors was defined by pairs of rectangular copper collimators mounted on the outside of an evacuated box. The collimators were 1.000 in. high, 0.500 in. wide, 0.156 in. thick and were located 7.00 and 24.00 in. from the center of the gas cell. An antiscattering baffle 1.25 in. high and 1.00 in. wide was placed halfway between the defining apertures. For forward angles a single detector system with smaller angular acceptance was used to reduce the length of the gas path observed. For this arrangement the copper collimators were 0.500 in. high by 0.250 in. wide and their distances to the target center were 7.50 and 25.00 in., respectively.

The measurements were made with gas pressures in the range of 15–30 in. of mercury, except at the forward angles where lower gas pressures were used to diminish the effects of multiple scattering. The target gas was research-grade natural oxygen of 99.9% purity. Several flushings of the gas cell before each series of measurements insured that the total initial impurity of the gas was less than 0.3%. To prevent contamination buildup during the measurements the cylindrical gap of the gas cell was covered by two foils made of Kapton H film.[18] The outer foil was 0.002 in. thick and the inner foil was 0.001 in. thick. The volume between the two foils was maintained at a low pressure and acted as a buffer volume.

The scintillation detectors consisted of NaI(Tl) crystals (2 in. diam, 0.5 in. thick) optically coupled to RCA-8053 photomultiplier tubes. The amplified signals from the photomultiplier tubes were processed by an SDS 925 on-line computer operating in a 4×512 channel, single-parameter mode. The over-all energy resolution was typically 1.5% for 46-MeV protons.

B. Energy Spectra

A spectrum of protons scattered from the oxygen gas target is shown in Fig. 1 along with an energy level diagram.[19] The first two peaks below the elastic peak, which are not completely resolved, each contain contributions from two levels, 6.05 MeV (0^+), 6.13 MeV (3^-) and 6.92 MeV (2^+), 7.12 MeV (1^-), respectively. The clearly resolved 8.88-MeV (2^-) state is relatively strongly excited at all energies studied. The next three levels, 9.61 MeV (1^-), 9.85 MeV (2^+), and 10.35 MeV (4^+), are weakly excited. The group of levels between 10.95 and 11.63 MeV was strongly excited. A weakly excited level which corresponds to the 12.44-MeV (1^-) or the 12.53-MeV (2^-) state was observed at incident proton energies below 34.1 MeV. The data of Hornyak and Sherr[20] would indicate the latter to be the more probable choice. At least one of the four $T=1$ levels between 12.80 and 13.26 MeV is strongly excited. Above $E_p=36.8$ MeV the strength in this region of excitation is noticeably decreased.

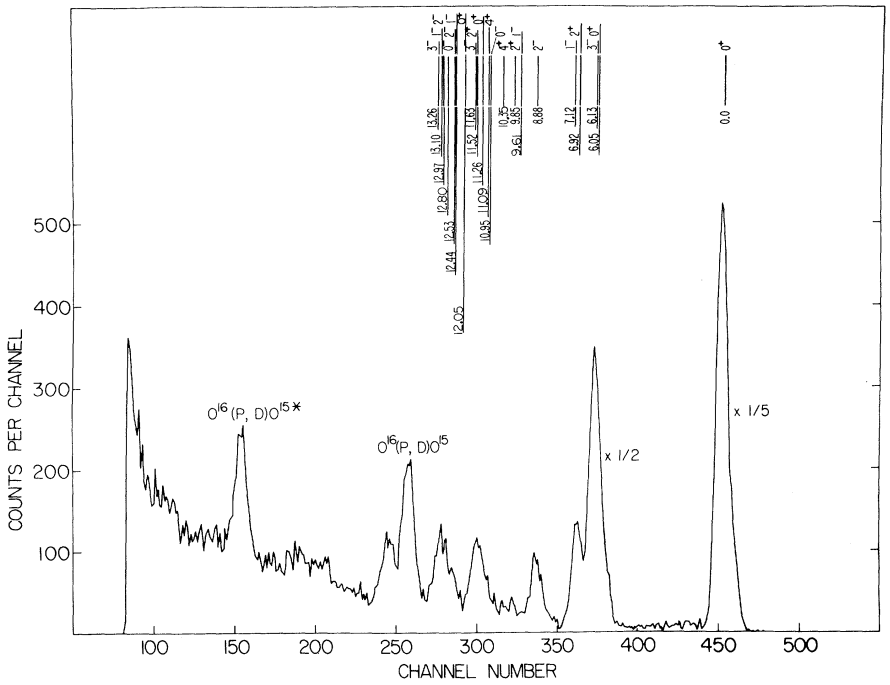

FIG. 1. Energy spectrum at $E_p = 34.1$ MeV, $\theta_{lab} = 40°$. The energy level diagram is taken from Ref. 19.

As can be seen in Fig. 1, the peaks sit on a continuous background which increases towards higher excitation energies. A nonnegligible contribution to the background stems from elastically scattered protons initiating nuclear reactions in the NaI(Tl) scintillation crystals.[21] In addition, the products of reactions having more than two bodies in the final state give rise to an increasing number of continua for increasing excitation energies. The highest energy end point is for the $^{16}O(p, p\alpha)$-^{12}C reaction, which has a Q value of -7.16 MeV.

C. Data Reduction

The peak near 6.1 MeV of excitation is a doublet consisting of states at 6.05 and 6.13 MeV, and it partially overlaps with the 6.92-7.12-MeV doublet. Fortunately the 6.92-7.12-MeV peak was less than $\frac{1}{4}$ the height of the 6.13-MeV peak at most angles, and it was possible to reliably extract the differential cross sections for the 6.05-6.13-MeV doublet. The 8.88-MeV peak was well resolved from other peaks and its analysis was straightforward.

To minimize subjective errors the spectra were analyzed using an automatic peak-stripping routine. The peaks were assumed to be of Gaussian form and the background function consisted of a combination of linear and exponential terms. The linear term was calculated by taking an average over a number of channels between the peaks corresponding to elastically scattered protons and protons scattered leaving the oxygen nucleus in its first excited state. The exponential and Gaussian functions were varied to minimize the quantity χ^2:

$$\chi^2 = \frac{1}{n-p} \sum_{i=1}^{n} \frac{(T_i - N_i)^2}{N_i},$$

where n is the number of data points and p is the number of free parameters. The number of events in the ith channel is denoted by N_i. The calculated number, T_i, is the sum of the contributions for the ith channel. In the analysis of the 8.88-MeV (2^-) state one Gaussian was used and therefore p was five. In the case of the doublet at 6.1 MeV two Gaussians were used due to the partial overlap with the doublet centered at 7.0 MeV and thus p was eight. The values obtained for χ^2 were typically 0.5 to 1.5. When the program produced larger values of χ^2 the results were not included in the angular distributions.

The relative errors in the differential cross sections for the 0^+-3^- doublet and the 2^- state are typically 5% for angles greater than 50° increasing to 10% at smaller angles. The relative uncertainties are mostly due to counting statistics and possible errors introduced by the peak-fitting routine.

In addition to the relative errors, there is an uncertainty of ±2.5% in the absolute scale. The largest contribution to this uncertainty is the fact that no corrections were made for protons which initiated nuclear reactions in the NaI(Tl) crystals. This correction varies as a function of proton energy and would increase the results of the measurements by less than 1.7% in this ener-

gy region.[21] The uncertainty due to finite geometry was estimated to be ±0.3% using an extended version[22] of Silverstein's formalism in order to allow for a rectangular beam profile. The absolute calibration of the current integration is accurate to ±1.0%. Other sources of relative and absolute error included in the above estimates are as discussed and evaluated in Ref. 17. The beam energy was determined to within ±0.2 MeV by means of the crossover technique.[23]

D. Experimental Results

The experimental angular distributions for the ^{16}O$(p,p')^{16}$O (8.88 MeV) reaction at 23.4, 24.5, 27.3, 30.1, 34.1, 36.8, 39.7, 43.1, and 46.1 MeV are shown in Fig. 2. Also shown are angular distributions at 17.0 and 18.8 MeV from Daehnick.[24] The most striking feature of the angular distributions is the nonmonotonic variation with energy below 30 MeV. At 23.4 MeV the angular distribution is nearly flat as observed at 18.8 MeV by Daehnick[24] and at 17.5 MeV by Crawley and Garvey.[25] However, at 24.5 MeV a pronounced minimum appears at about 115° in the c.m. system. This minimum is present at all higher energies. The general shape of the curves then remains constant up to 30.1 MeV, but between 30.1 and 36.8 MeV the differential cross section at backward angles noticeably increases. As the incident energy is raised above 36.8 MeV, a second minimum begins to form at about 90° c.m. Above 30 MeV there is

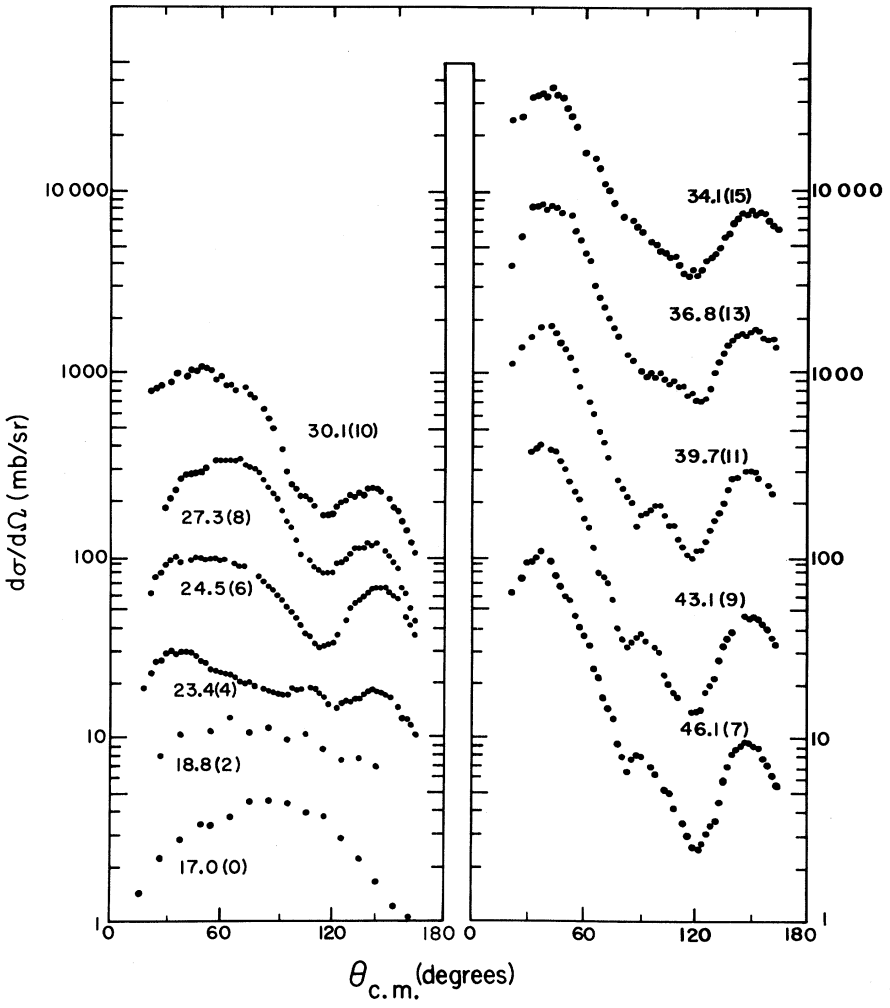

FIG. 2. Differential cross sections leading to the 8.88-MeV 2^- state in ^{16}O. The energies are given in MeV near each distribution. The number in parentheses following the energy is the power of 2 by which the plotted cross sections must be divided to obtain the true cross section. For example, the 30.1-MeV points must be divided by $2^{10}=1024$. The 17.0- and 18.8-MeV data are from Ref. 24 and the other data are the present work. Typical errors are ±10% for $\theta < 50°$ and ±5% for $\theta > 50\%$.

a smooth energy variation in the general shape.

Figure 3 shows the angular distributions of the 6.05-6.13-MeV doublet for the same incident proton energies. The ratio of the transitions to the 6.05-MeV state and the 6.13-MeV state is less than 1:8 between 20 and 90° at $E_p = 17.5$ MeV.[25] Between 24 and 40 MeV this ratio is less than 1:10 between 20 and 100°.[26] For an incident proton energy of 150 MeV[27] the ratio at a laboratory angle of 15° is equal to $1:(14^{+21}_{-6})$. Thus, at forward angles the angular distributions are essentially those for inelastic scattering to the 6.13-MeV (3^-) state. The shape of the angular distributions does not vary appreciably over the range of incident proton energies 27–46 MeV. Furthermore, the differential cross section for angles below 50° c.m. is approximately constant.

The total cross section for each of the two transitions was obtained by extrapolating the cross sections linearly to $\sigma(0°) = 0$ from the last measured point at small θ and to $\sigma(180°) = \sigma(\theta_{max})$, where $\sigma(\theta_{max})$ is the experimental cross section at the largest angle measured. The contribution from the extrapolated region was usually 3–7% except at 36.8 MeV where it was 13% for the 6.1-MeV transition, and at 43.1 MeV where it was 18% for the 8.88-MeV transition. The total cross sections are shown in Fig. 4. The errors shown are total errors and include an uncertainty of $\frac{1}{2}$ the cross section in the extrapolated region.

Excitation functions for $^{16}O(p,p')$ have been measured up to 40 MeV.[15] Relatively narrow peaks in the excitation functions were observed at backward angles up to about 27 MeV. Thus, compound-nucleus processes may be responsible for the rapid changes in the shape of the 8.88-MeV angular

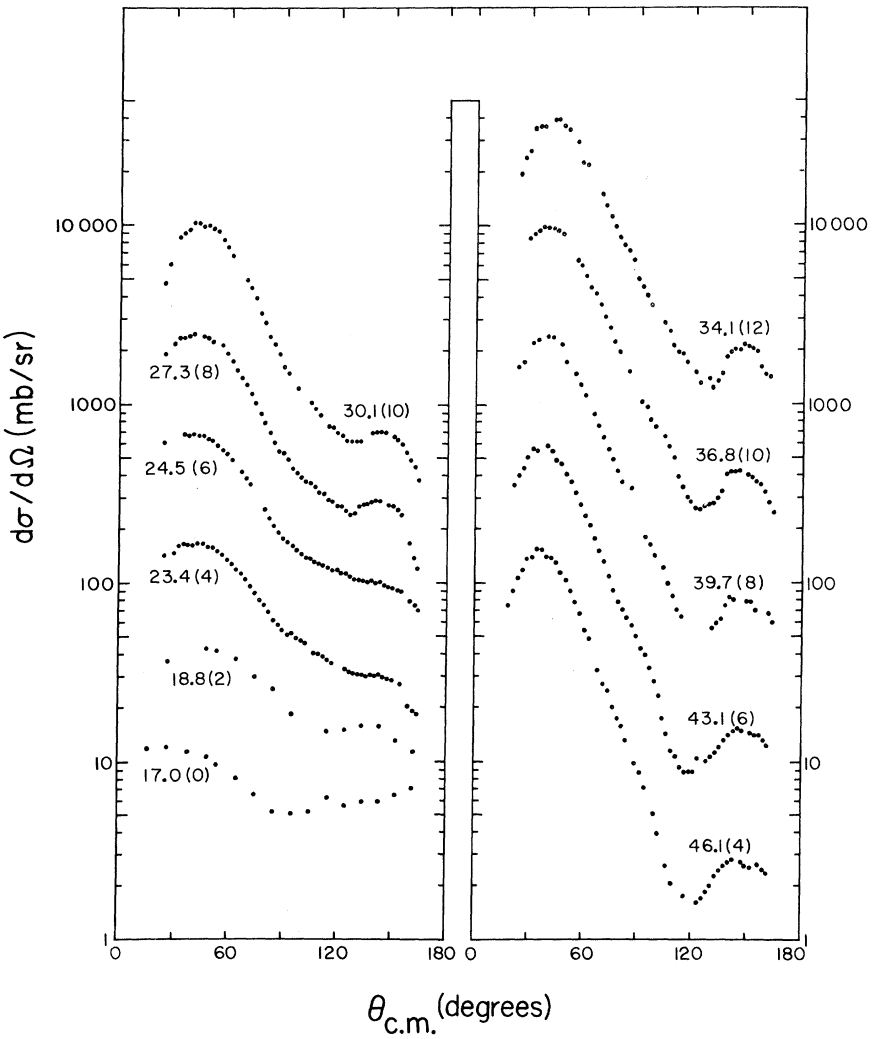

FIG. 3. Differential cross sections leading to the doublet of states near 6.1 MeV in ^{16}O(6.05 MeV, 0^+ and 6.13 MeV, 3^-). For other details see the caption of Fig. 2.

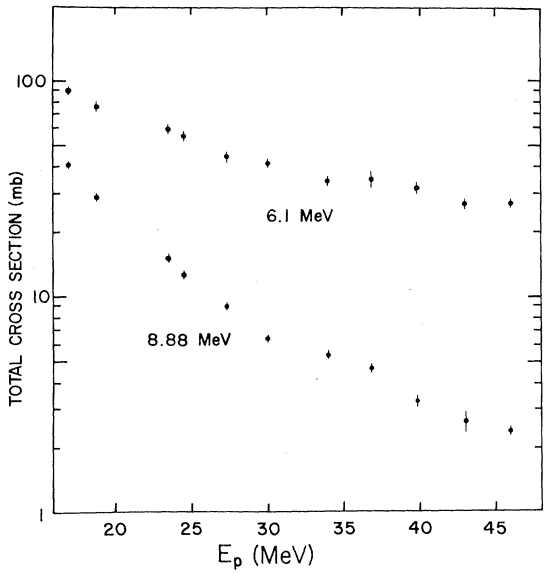

FIG. 4. Total cross sections for the 6.1- and 8.88-MeV transitions obtained by integrating over the differential cross sections shown in Figs. 2 and 3. See the text (Sec. II D) for details.

distributions for bombarding energies less than 25 MeV. The decreasing importance of compound-nucleus formation is presumably the reason for the rapid decrease observed in the total cross sections for both the 6.1- and 8.88-MeV transitions as the incident energy is increased towards 30 MeV. There is no clear evidence for nondirect processes at proton energies above 30 MeV. It should be noted that even above 30 MeV the total cross section for the 8.88-MeV transition decreases more rapidly than that for the 6.1-MeV transition. This behavior has been previously observed by Benenson and Crawley[28] in measurements of the deexcitation γ rays from these levels. A possible explanation of this effect will be discussed in Sec. IV.

III. THEORETICAL ANALYSIS

A. Outline of the Theory

In the local DWA theory of inelastic scattering the transition amplitude can be written[1]

$$T_{fi} = \int \chi_f^{(-)*} \langle \psi_f | V_{\text{eff}} | \psi_i \rangle \chi_i^{(+)} d\vec{r} .$$

In this expression χ_f and χ_i are distorted waves generated from a phenomenological optical-model potential deduced by fitting the elastic scattering data. The form factor $\langle \psi_f | V_{\text{eff}} | \psi_i \rangle$ contains all the nuclear-structure information. In a microscopic description of the reaction the wave functions ψ_f and ψ_i represent shell-model states. The effective interaction V_{eff} which causes transitions between these states is taken to be[1]

$$V_{\text{eff}} = \sum_i t_{ip} ,$$

where t_{ip} describes the scattering of the projectile p from the ith target nucleon and where the sum is over the nucleons of the target nucleus. If only central forces contribute to the interaction, one can approximate t_{ip} by

$$t_{ip} = V_{00} + V_{10} \vec{\sigma}_i \cdot \vec{\sigma}_p + V_{01} \vec{\tau}_i \cdot \vec{\tau}_p + V_{11} (\vec{\sigma}_i \cdot \vec{\sigma}_p)(\vec{\tau}_i \cdot \vec{\tau}_p) . \tag{2}$$

Here $\vec{\sigma}_i$ and $\vec{\sigma}_p$ are the Pauli spin operators for the target nucleon and the projectile, respectively, and $\vec{\tau}_i$ and $\vec{\tau}_p$ are the analogous isospin operators. The subscripts on the V_{ST} are the transferred spin and isospin. For inelastic scattering to states of zero isospin in a self-conjugate nucleus, only the first two terms of the sum contribute. Possible effects of noncentral terms in t_{ip} will be discussed in Sec. IV.

B. Optical-Model Potentials

Cross-section and polarization angular distributions for the elastic scattering of protons from ^{16}O had been obtained at all energies of this experiment.[17,29] The optical-model potentials derived by fitting both polarization and cross-section data have been published elsewhere.[30] The form of the optical model used in this analysis using the notation of Ref. 30 is given by

$$U(r) = V_C(r) - V \frac{1}{1+e^{x_1}} - iW \frac{1}{1+e^{x_2}} - iW_1 e^{-x_3^2} + (V_s + iW_s) \frac{4}{r} \frac{d}{dr} \frac{1}{1+e^{x_4}} (\vec{s} \cdot \vec{l}) . \tag{3}$$

The x_i are related to the diffuseness and radius parameters according to

$$x_1 = (r - r_0 A^{1/3})/a , \quad x_2 = (r - r_i A^{1/3})/a_i , \quad x_3 = (r - r_i A^{1/3})/b_i , \quad x_4 = (r - r_s A^{1/3})/a_s . \tag{4}$$

The relevant optical-model parameters for the DWA analysis are given in Table I.

One modification had to be introduced in the calculation of the distorted waves. The potential used in the DWA program contained a surface imaginary central potential of the derivative Woods-Saxon type

$$iW_D \times 4a_D \frac{d}{dr} \frac{1}{1+e^{x_5}} , \quad x_5 = \frac{r - r_i A^{1/3}}{a_D} , \tag{5}$$

while that used in the optical-model analysis had a Gaussian shape [see Eq. (3)]. It was assumed that the derivative Woods-Saxon potential had the same strength and width at half maximum as the Gaussian potential: thus $W_1 = W_D$, $a_D = 0.472 b_i$.

TABLE I. UM-UCLA optical-model parameters. [See Ref. 30. The notation follows that of Eqs. (3) and (4).] The potential strengths are given in MeV.

E_p (MeV)	V [a]	W	W_1	V_s
23.4	47.25	0.00	7.06	−4.09
24.5	44.51	0.00	6.83	−5.41
27.3	48.43	0.00	7.28	−5.63
30.1	47.50	0.00	8.35	−6.82
34.1	47.02	2.31	6.52	−6.44
36.8	46.37	0.28	8.55	−7.98
39.7	46.58	2.25	7.65	−7.32
43.1	44.67	3.15	6.32	−6.20
46.1	42.13	4.44	4.64	−6.20

[a]The geometrical parameters are $r_0 = 1.142$ F, $r_i = 1.268$ F, $r_s = 1.114$ F, $a = 0.726$ F, $a_i = 0.676$ F, $a_s = 0.585$ F, and $b_i = 1.45\ a_i$.

As is common in light nuclei, it was not possible to obtain good simultaneous fits to the elastic scattering differential-cross-section and polarization data, although they could be fitted fairly well separately.[30,31] To estimate the effects of this ambiguity on the DWA calculations, distorted waves generated from optical-model potentials derived by Snelgrove and Kashy[32] from fits to their differential-cross-section data in this energy range were also used. These potentials are given in Table II.

The optical potentials for the exit channel were the same as those for the entrance channel, except that the real potential strength was determined using

$$V(\text{exit}) = V(\text{entrance}) + 0.33 \times \tfrac{17}{16}|Q|$$

to account for the energy dependence of the potential. The slope $dV/dE = -0.33$ is consistent with the analysis of van Oers and Cameron[30] and Snelgrove and Kashy[32] in this energy range.

C. Effective Interaction and Wave Functions

The radial dependence of the effective interaction was assumed to be Yukawan with an inverse range α and was given by the relation

$$V_{10} = V_\sigma \frac{e^{-\alpha r}}{\alpha r}, \quad V_{00} = V_C \frac{e^{-\alpha r}}{\alpha r}. \tag{6}$$

Earlier calculations[8] have shown that a range $\alpha^{-1} = 1.0$ F is approximately correct for a Yukawan radial dependence, and this value for the range was used throughout the analysis except for a few test cases. The magnitude of the inelastic scattering cross section is proportional to V_σ^2 or V_C^2 and these strengths can be determined by fitting the data.

The data were also compared with cross sections determined using an IA pseudopotential derived by Petrovich *et al.*[33-36] from the free two-nucleon interaction. This pseudopotential also has a Yukawan radial dependence, but it is complex and both the range and strength vary with energy. Typical values of the parameters are given in Table III.

TABLE II. MSU optical-model parameters. [Obtained by extrapolation from the results of Ref. 32 at 25.46, 32.07, 35.20, 38.43, and 45.13 MeV. The notation follows that of Eqs. (3)–(5).] The potential strengths are given in MeV; r_i and a_D are given in F.

E_p (MeV)	V [a]	W	W_D	V_s	r_i	a_D
24.5	49.50	0.00	7.20	−7.00	1.155	0.560
27.3	47.55	0.00	6.20	−7.00	1.260	0.532
30.1	46.45	0.00	5.50	−7.00	1.365	0.505
39.7	43.80	2.30	5.45	−7.00	1.375	0.425
46.1	42.50	3.20	5.70	−7.00	1.250	0.415

[a]The geometrical parameters which were held constant are $r_0 = 1.12$ F, $r_s = r_0$, $a = 0.69$ F, and $a_s = a$.

The wave functions used in the calculations for the 2^- and 3^- states in ^{16}O were those of the lowest-lying states of that spin and parity resulting from the calculations of Gillet and Vinh Mau.[14] Harmonic-oscillator radial wave functions were used with the oscillator parameter $a = 1.76$ F, chosen to fit electron elastic scattering data.[37]

D. Calculations for the 8.88-MeV (2^-) State

The form factors were calculated and inserted into a DWA code which allows the use of spin-orbit coupling in the optical potentials.[38] The selection rules allow two amplitudes to contribute to the 2^- transition. These amplitudes add coherently and correspond to transferred quantum numbers $(LSJT) = (1120)$ and (3120). Calculations including both amplitudes were performed at $E_p = 30.1$ and 46.1 MeV, and it was found that the (3120) amplitude contributed less than 3.5% to the cross section at any angle. Therefore, all subsequent calculations included only the contribution of the (1120) amplitude.

The results of calculations at 27.3, 39.7, and 46.1 MeV are shown in Figs. 5–7. Each of these

TABLE III. Impulse-approximation values for V_{10}. (See Ref. 35. The form of V_{10} is $V_{10}(r) = V_{\sigma R}\, e^{-\beta r}/\beta r + iV_{\sigma I}\, e^{-\gamma r}/\gamma r$.

E_p (MeV)	$V_{\sigma R}$ (MeV)	β (F^{-1})	$V_{\sigma I}$ (MeV)	γ (F^{-1})
27.3	146	2.5	19	1.50
39.7	98	2.5	13	1.64
46.1	80	2.5	12	1.80

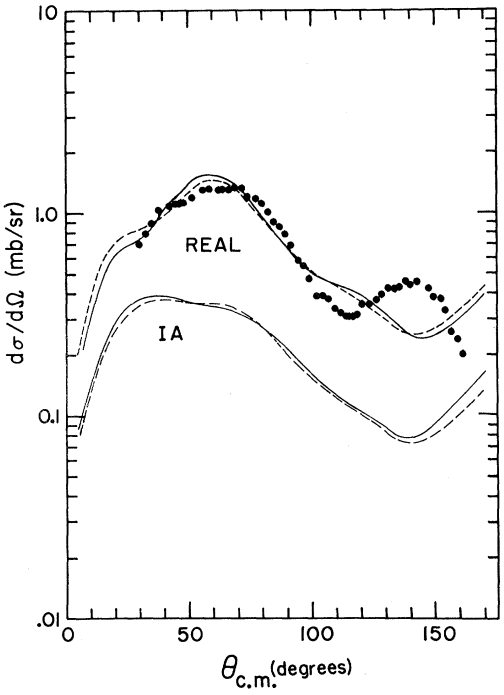

FIG. 5. Comparison of the 8.88-MeV angular distribution at E_p=27.3 MeV with DWA calculations. The upper two curves are for the real interaction of Eq. (6) with α =1.0 F^{-1} and the lower two curves are for the impulse approximation of Refs. 34 and 35 as given in Table III. The dashed and solid curves were calculated with the MSU and UM-UCLA optical-model potentials, respectively. See the text (Secs. III B and III D) for details.

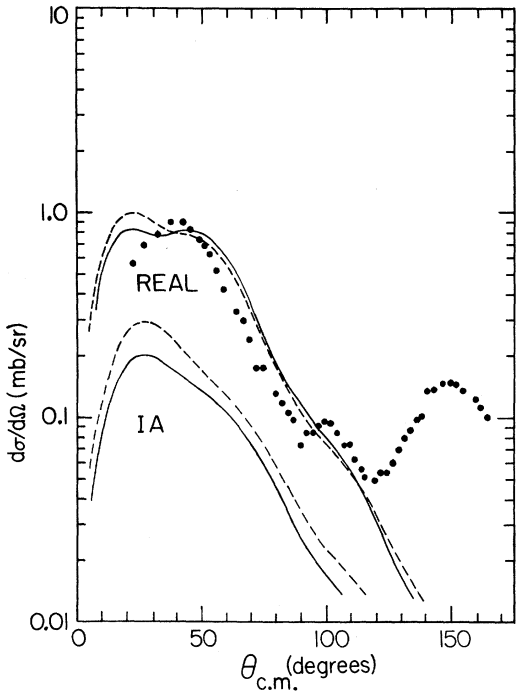

FIG. 6. Comparison of the E_p=39.7-MeV angular distribution for the 8.88-MeV state with DWA calculations. See Fig. 5 for details.

figures contains four curves. The lower two curves were calculated using the IA pseudopotential of Petrovich *et al.*,[33-36] which contains no adjustable parameters. The upper two curves were calculated using the real interaction of Eq. (6), with the strength of the interaction adjusted to make the calculated total cross section equal to the experimental total cross section shown in Fig. 4. The solid curves were calculated with the optical-model potentials of van Oers and Cameron[30] (UM-UCLA potentials) while the dashed curves were calculated with those of Snelgrove and Kashy[32] (MSU potentials).

The resulting values of V_σ are shown in Fig. 8. The closed circles were obtained with the UM-UCLA potentials and the open circles were obtained with the MSU potentials. The points at low energy were calculated from the data of Crawley and Garvey[25] at 17.5 MeV and from the data of Daehnick[24] at 17.0 and 18.8 MeV using optical-model potentials derived from the elastic scattering cross sections at 17.5 MeV.[39] The points labeled impulse approximation, calculated using the UM-UCLA potentials, are the values of V_σ for a

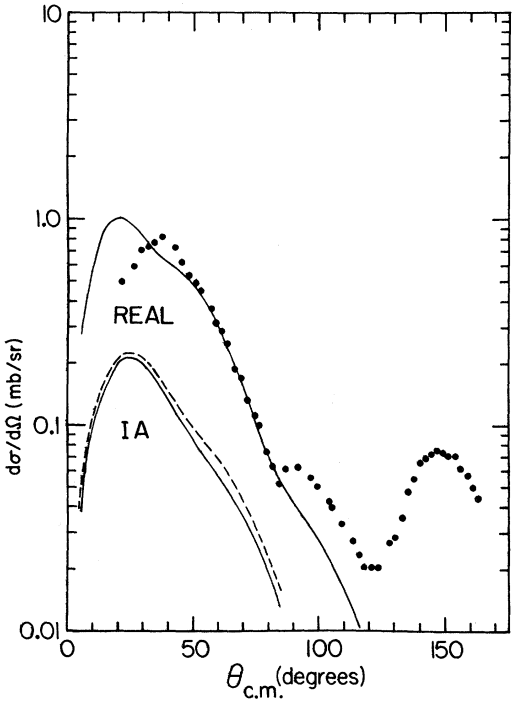

FIG. 7. Comparison of the E_p=46.1-MeV angular distribution for the 8.88-MeV state with DWA calculations. See Fig. 5 for details. The calculations using the real interaction of Eq. (6) were indistinguishable for the MSU and UM-UCLA optical-model potentials.

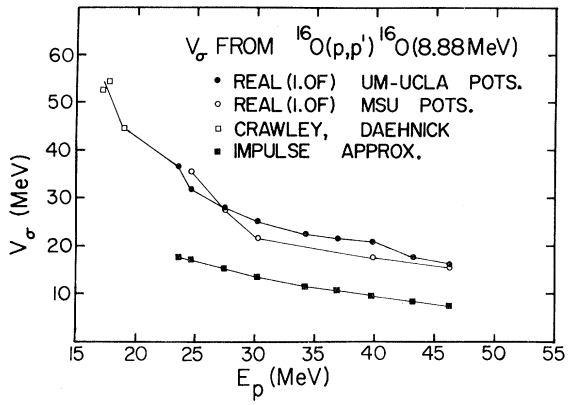

FIG. 8. The strength of the spin-dependent part of the two-nucleon interaction. For details see the text (Sec. III D).

real interaction of Yukawan shape with 1.0 F range which produces the same total cross section as the IA interaction.

E. Calculations for the 6.1-MeV Doublet

Calculations were performed at $E_p = 30.1$ and 46.1 MeV using both the IA pseudopotential and a real interaction with the form of Eq. (6). Amplitudes with $(LSJT) = (3030)$ and (3130) are allowed by the selection rules. While in principle these amplitudes can add coherently, they are in fact essentially incoherent.[26] The cross section for the (3130) amplitude was evaluated using the strengths V_σ shown in Fig. 8 and was only 1% of the experimental cross section at 30.1 and 46.1 MeV. The spin-flip amplitude was therefore neglected and the cross sections were calculated using the (3030) amplitude only. For the real interaction, V_C was determined by matching the calculated and experimental total cross sections, assuming that the entire experimental cross section was due to the 6.13-MeV (3^-) state. The results of the analysis are given in Figs. 9 and 10 and in columns 2 and 4 of Table IV.

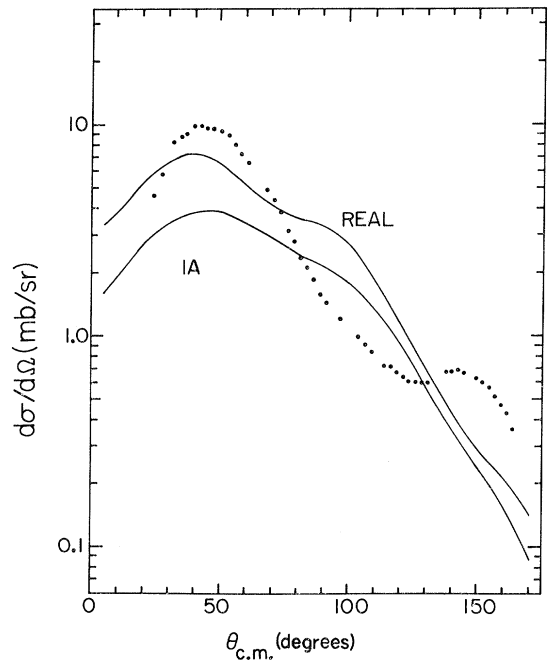

FIG. 9. Comparison of the $E_p = 30.1$-MeV angular distribution for the 6.1-MeV doublet with DWA calculations performed assuming only the 6.13-MeV 3^- state has an appreciable cross section. The top curve is for the real interaction of Eq. (6) with $\alpha = 1.0$ F^{-1} and the bottom curve is calculated with the impulse approximation of Refs. 34 and 35. The UM-UCLA optical-model potentials were used.

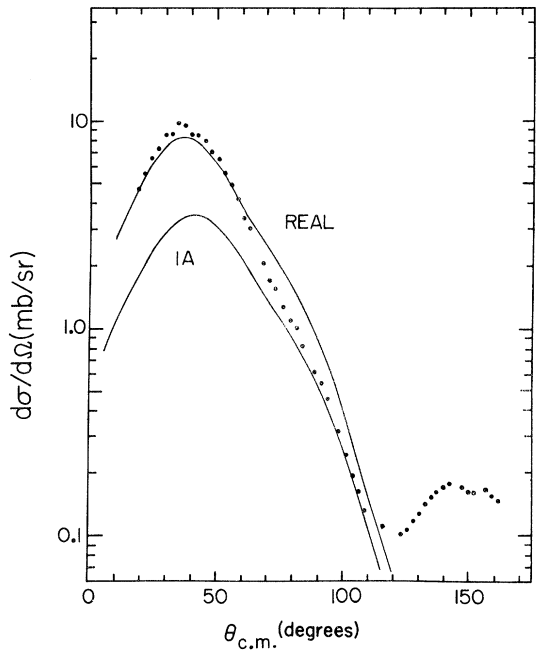

FIG. 10. Comparison of the $E_p = 46.1$-MeV angular distribution for the 6.1-MeV doublet with DWA calculations. For details see Fig. 9.

TABLE IV. Values of V_C and $V_{C,eq}$ obtained from the 6.13-MeV angular distributions. $V_{C,eq}$ is a real potential which predicts the same total cross section as the impulse-approximation effective interaction.

E_p (MeV)	V_C [a] (MeV)	V_C [b], corrected (MeV)	$V_{C,eq}$ [a] (MeV)
30.1	85	65	67
46.1	74	57	51

[a] For the potential of Eq. (6) with $\alpha = 1.0$ F^{-1}.

[b] The values in column 3 were obtained by multiplying those of column 2 by $(1/1.7)^{1/2}$. See Sec. IV B.

IV. DISCUSSION

A. 8.88-MeV (2^-) Transition

Perhaps the most surprising aspect of the results shown in Figs. 5–8 is the amount by which the IA underestimates the total cross section. At all energies the ratio of the experimental cross section (σ_{EXP}) to the IA prediction (σ_{IA}) lies in the range $\sigma_{EXP}/\sigma_{IA} = 4.0 \pm 0.7$. Petrovich *et al.*[34,35] have shown that the IA accounts for the strong $S=0$, $T=0$ transitions induced by V_{00} if one uses wave functions which properly describe the collective properties of the states involved. The IA also predicts the cross sections for transitions induced by V_{11} to within a factor of 2 at incident energies above 30 MeV.[2] Thus it is somewhat unexpected that the IA fails so badly in this case. In the present calculations space exchange has been neglected. This presumably does not affect the results of the IA calculations, since the IA pseudopotential was obtained[34,35] from a nucleon-nucleon scattering amplitude which was calculated including exchange of the two nucleons. Petrovich[35] has shown that this treatment is approximately equivalent to using a potential which fits the nucleon-nucleon scattering and including exchange effects in the DWA calculation.

Another unexpected result is that the fits deteriorate at the higher energies where one would expect the DWA to reproduce more closely the experimental data. The predicted peak in the cross section occurs at smaller angles than the observed peak. In the next few paragraphs we discuss the sensitivity of the calculations to changes in the parameters of the model in an attempt to understand these discrepancies.

Since it is known[14] that the RPA wave functions used in the present calculations do not provide a particularly good description of the 2^- state, we have investigated the sensitivity of the predictions to the less important configurations in the wave functions. Calculations were made at 30.1 MeV in which the wave functions of Gillet and Vinh Mau[14] were replaced by wave functions containing only the dominant configuration, $(1p_{1/2}^{-1}, 1d_{5/2})$. The resulting cross section is indistinguishable in shape from that calculated using the complete wave functions but is larger in magnitude by a factor of 1.42. This is in contrast to the case of $S=T=0$ transitions which are strongly enhanced by the less important configurations in the wave function. If the same effect is assumed at all energies, the use of the simple wave functions defined above would reduce σ_{EXP}/σ_{IA} to 2.8 ± 0.5 and reduce the values of V_σ of Fig. 8 by a factor of $1.42^{1/2}$.

Calculations were performed with the range given by $\alpha^{-1} = 0.7$ F and $\alpha^{-1} = 1.4$ F to compare with the standard calculations for which $\alpha^{-1} = 1.0$ F. The results at 46.1 MeV are shown in Fig. 11. It is clear that reasonable changes in α^{-1} cannot account for the observed behavior of the cross section. The results shown in Fig. 11, as well as a similar calculation at 27.3 MeV, permit a determination of a scaling relationship for V_σ as a function of α^{-1} in the range 0.7–1.4 F, which can be expressed as

$$V_\sigma(\alpha)/V_\sigma(\alpha') = (\alpha/\alpha')^{2.4}.$$

This result applies only to the reaction considered here.

Calculations were also performed at 30.1 MeV with the harmonic-oscillator parameter set equal to 2.13 and 1.49 F for comparison with the results for the canonical value of $a = 1.76$ F. The angular distribution did not change significantly except that for a value of $a = 2.13$ F a subsidiary peak developed near 20°. The total cross section at these extreme values of a changed by −11% (2.13 F) and +15% (1.49 F).

Finally, there are changes associated with different optical-model potentials. As can be seen from Figs. 5–8, the shapes of the angular distributions are weakly affected by changes in potentials which are consistent with the elastic scattering data. However, the total cross sections change by as much as 30%. Because the spin-orbit potentials are probably the least accurately de-

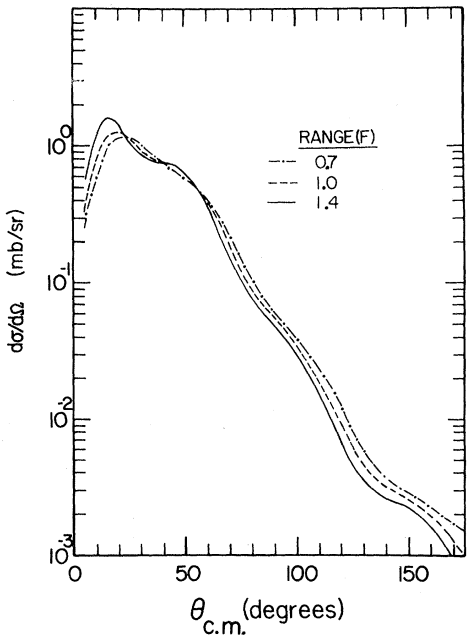

FIG. 11. DWA calculations for the 8.88-MeV state with several values of the range α^{-1} of V_{10}.

TABLE V. Values of V_σ from (p, p') reactions.

Target	Final state (MeV)	E_p (MeV)	Interaction	V_σ [a] (MeV)
^{16}O [b]	2^-, 8.88	17.5	V_σ	53
^{32}S [b]	1^+, 4.70	17.5	V_σ	53
^{89}Y [c]	$\frac{3}{2}^-$, 1.51	24.5	$V_\sigma+V_{\sigma\tau}$	<23
^{89}Y [d]	$\frac{9}{2}^+$, 0.908	61.2	$V_\sigma+V_{\sigma\tau}$	≅7
^{89}Y [d]	$\frac{3}{2}^-$, 1.51	61.2	$V_\sigma+V_{\sigma\tau}$	<12
^{208}Pb [e]	4^-, 3.475	61.2	$V_\sigma-V_{\sigma\tau}$	23.5
$1p$ shell [f]				15.6
$2s$-$1d$ shell [f]				23.3

[a] For $\alpha^{-1}=1.0$ F.

[b] Data of Ref. 25 as analyzed in Ref. 9. V_σ was converted from the value for a 1.7-F Gaussian shape (Ref. 9) to a 1.0-F Yukawa shape by requiring that the volume integrals be equal.

[c] See Ref. 12.

[d] See Ref. 13.

[e] See Ref. 10.

[f] See Ref. 40.

termined part of the optical-model potentials, calculations have been performed with $V_s = 0.0$ MeV. At 46.1 MeV the shape is changed only slightly and the total cross section is decreased by 19%. One can conclude that reasonable changes in the parameters do not explain the discrepancy in either the shapes of the angular distributions at the higher energies or in the magnitude of the total cross section.

Other values of V_σ from the literature are listed in Table V. In some of these cases the cross section is sensitive to $V_{10} \pm V_{11}$. To obtain the values of V_σ shown in column 5, the strength of V_{11} $(V_{\sigma\tau})$ is set equal to 13 MeV. The relative signs of V_{10} and V_{11} have not yet been fixed by experiment and the signs chosen here are the prediction of the IA.[33-36] The last two rows in the table contain results obtained by Schmittroth[40] from shell-model calculations for the $1p$ and $2s$-$1d$ shells.

B. 6.13-MeV (3^-) Transition

The shapes of the calculated angular distributions match the data rather poorly at 30.1 MeV, but at 46.1 MeV the agreement is reasonably good. The agreement improves because of the change in the shape of the calculated angular distributions, since the shapes of the experimental angular distributions remain almost constant over this energy range.

The ratio σ_{EXP}/σ_{IA} equals 1.6 at 30.1 MeV and 2.1 at 46.1 MeV. At 46.1 MeV the shapes of the experimental and theoretical angular distributions agree well enough that a normalization to the peak in the differential cross section at 35° c.m. is reasonable $[\sigma_{EXP}(\text{peak})/\sigma_{IA}(\text{peak}) = 2.7]$. Recently Bergstrom *et al.*[41] have compared their inelastic electron scattering data for the 6.13-MeV state to differential cross sections obtained by Gillet and Melkanoff[42] with the same RPA wave functions as used in the present analysis. The measured cross sections exceed the predictions by a factor of about 1.7 for the entire range of momentum transfers (q).

Since the discrepancy is independent of q, one can conclude that the radial transition density[42] is too small by a factor of $(1.7)^{1/2}$. The same transition density also appears in the expression for inelastic proton scattering[35] and contains all the important nuclear-structure information. Thus, one can correct for the inadequacy of the wave functions used in the present analysis by multiplying the DWA cross sections by 1.7.

Applying this correction to the IA prediction yields $\sigma_{EXP}(\text{peak})/\sigma_{IA}(\text{peak}) = 1.6$. Since the cross section is proportional to the square of the strength of the interaction, the IA gives the strength of the effective interaction to within 25% at $E_p = 46.1$ MeV. If one compares total instead of peak cross sections, with this correction the strength of the IA effective interaction is correct within 11% at $E_p = 30.1$ and 46.1 MeV. The values for the strength of the real interaction corrected in the same way are given in column 3 of Table IV.

As was noted above, space exchange is approximately included in the IA calculations, but it is neglected in the calculations with the real force of Eq. (6). It has been found[33] that the inclusion of exchange processes enhances the cross section for the $^{12}C(p,p')^{12}C$ (9.64 MeV, 3^-) reaction at $E_p = 45.5$ MeV by a factor of 4. A similar enhancement is expected in the present case, since the states have the same quantum numbers and roughly the same shell-model orbits. Thus it is likely that the strengths in Table IV would be reduced by about a factor of 2 if exchange were included in the DWA calculation.

C. Energy Dependence of Total Cross Sections

As previously noted the total cross section for the 8.88-MeV transition decreases much more rapidly with increasing incident proton energy than does the total cross section for the 6.13-MeV transition. Below 30 MeV it is reasonable to attribute this behavior to the decreasing importance of compound-nucleus formation. At the higher energies, however, direct-reaction processes predominate and a more attractive explanation is contained in the observation of Petrovich[43] that the cross section for a transition will decrease rapidly with increasing energy if the transition is mediated by a long-range force. An explanation of the observed

behavior is that V_{10} has a longer range than V_{00}. The spin-dependent part of the free nucleon-nucleon force also appears to have a long range, since V_{10} is the most rapidly varying part of the IA pseudopotential[34] which was derived from the Hamada-Johnston[44] potential (see Table III). This rapid energy dependence is evident in Fig. 8 where the IA prediction of V_σ, while too small, decreases even more rapidly than the experimentally determined value of V_σ.

It is the rapid decrease in the exchange part of the cross section which accounts for most of the decrease in the cross section with increasing energy.[43] Since the present calculation neglects exchange, one expects to find that V_σ also decreases. This is consistent with the data shown in Fig. 8, but it is not clear how much of the observed decrease can be attributed to this effect.

D. Other Reaction Mechanisms

In the analysis of Sec. III it was assumed that the reaction was dominated by the direct spin-flip process. However, the ^{16}O$(\alpha, \alpha')^{16}$O reaction is observed to populate the 2^- state[16] and since spin-flip cannot occur for spin-zero particles, other reaction processes must exist which may contribute to the (p, p') cross sections discussed here. These processes can include[16] (i) processes induced by a tensor interaction or by a spin-orbit interaction between the orbital angular momentum of the incident particle and the spin of the valence nucleons of the target, (ii) space-exchange processes in which L need not satisfy the selection rule $\Delta\pi = (-1)^L$, (iii) compound-nucleus formation, and (iv) multiple-excitation processes in which the excitation proceeds through an intermediate state which is strongly excited by inelastic scattering [presumably the 6.13-MeV (3^-) state for ^{16}O].

There are no calculations of the first two effects relevant to ^{16}O, but it appears likely[16,40,45] that these effects do not strongly influence the cross section. Compound-nucleus formation is probably important in ^{16}O$(\alpha, \alpha')^{16}$O (8.88 MeV, 2^-), since the cross section has rapid irregular variations in both shape and magnitude up to at least $E_\alpha = 42$ MeV.[46] As has been noted above, compound-nuclear effects are not observed in ^{16}O(p, p') above $E_p = 30$ MeV.

It has been argued[28,47] that if a cross section decreases rapidly with increasing energy as is observed for the 8.88-MeV transition, it is an indication that second-order processes are important. It was not possible to test this argument for ^{16}O, since available coupled-channels codes assume a collective model for the wave functions of the nuclear states and such wave functions do not properly describe the states involved. However, cross sections are available for the ^{24}Mg$(\alpha, \alpha')^{24}$Mg (5.22 MeV, 3^+) reaction at $E_\alpha = 50.0$, 65.7, 81.0, and 119.7 MeV.[48] The cross sections leading to the 3^+ unnatural-parity state are well explained by a multiple-excitation process.[48] The differential cross sections for the 5.22-MeV transition and for the transition to the strongly excited 2^+ state at 1.369 MeV have been integrated and the ratio $\sigma(5.22)/\sigma(1.369)$ decreases slightly less than a factor of 2 between 50.0 and 119.7 MeV. The ratio $\sigma(8.88)/\sigma(6.13)$ for ^{16}O decreases about four times more rapidly for proton energies between 30.1 and 46.1 MeV. Thus, it appears that multiple-excitation processes do not necessarily cause a rapidly decreasing cross section and in the case of ^{16}O$(p, p')^{16}$O (8.88 MeV, 2^-) one may interpret the observed decrease as a further manifestation of the long range of V_{10}.

Evidence that different processes are responsible for the ^{16}O$(p, p')^{16}$O (8.88-MeV, 2^-) cross section and the cross sections for (α, α') leading to unnatural-parity states in ^{16}O(8.88 MeV, 2^-), ^{20}Ne (4.97 MeV, 2^-), and ^{24}Mg (5.22 MeV, 3^+) appears when one plots the cross sections as a function of momentum transfer. The (α, α') cross sections are found to vary irregularly as the energy is changed,[48] while the (p, p') cross sections have essentially identical shapes above 30.1 MeV as one expects for a direct process.

A possible experimental evaluation of the importance of processes which do not proceed through spin-flip would be recorded only those ^{16}O$(p, p')^{16}$O (2^-, 8.88-MeV) events which are in coincidence with an 8.88-MeV deexcitation γ ray emitted at 90° to the reaction plane. Such events correspond to no-spin-flip in the total process,[49] so that if one could disentangle the spin-flipping effects of the optical-model potential, one would have a measure of the $S = 0$ part of the cross section. Unfortunately, the γ-ray branch to the ground state is only about 7% of the total decays[50] so the experiment would be difficult.

V. SUMMARY

The cross sections for inelastic proton scattering to the 6.13-MeV (3^-) and 8.88-MeV (2^-) states of ^{16}O have been measured at nine energies between 23.4 and 46.1 MeV. The measured cross sections have been compared with a microscopic model of the reaction using both IA and real interactions. The IA predictions are too small by a factor of about 4 for the spin-flip transition to the 2^- state if RPA wave functions are used to describe the state. The cross sections for the RPA wave functions are smaller by a factor of 1.42 than

those calculated with a simple $(1p_{1/2}^{-1}, 1d_{5/2})$ configuration. The strength of the real interaction with a 1.0-F range was obtained by normalizing to the experimental total cross sections and was found to decrease from 23 MeV at $E_p = 30.1$ MeV to 16 MeV at $E_p = 46.1$ MeV. The rapid decrease of the cross section for excitation of the 2^- state with increasing energy was interpreted as an indication that the spin-dependent interaction V_{10} has a long range.

The shape of the angular distribution for the 6.13-MeV transition is fairly well described by the IA at 46.1 MeV but not at 30.1 MeV. However, at both energies the magnitude of the IA cross section is too small by about a factor of 2. Part of this discrepancy can be attributed to deficiencies in the RPA wave functions, since the predicted electron scattering cross sections are also too small. One can conclude that the IA pseudopotential describes the effective interaction within 10–25% depending on whether one fits the total or peak cross sections.

It is possible that small changes in the details of the calculation could improve the present somewhat unsatisfactory fits to the data. However, any interpretation must be tentative until a proper coupled-channels calculation is performed.

VI. ACKNOWLEDGMENTS

We would like to thank D. C. Larson for performing some of the DWA calculations and F. Petrovich for illuminating discussions. The calculations involved in analyzing the experimental data were performed using the computing facilities of the University of California, Los Angeles, Campus Computer Network and the University of Manitoba Institute for Computer Studies. One of the authors (SMA) wishes to thank the Aspen Center for Physics for its hospitality.

---

*Research supported in part by the National Science Foundation.

†Present address: Centre d'Etudes Nucléaires de Grenoble, Grenoble, France.

‡Present address: Department of Physics, University of Manitoba, Winnipeg, Canada.

§Present address: Department of Physics, University of Washington, Seattle, Washington 98105.

‖Research supported in part by the U. S. Atomic Energy Commission, Contract No. AT(11-1)-GEN 10 P. A. 18.

**Research supported in part by the Atomic Energy Control Board of Canada.

[1]G. R. Satchler, Nucl. Phys. 77, 481 (1966); V. A. Madsen, *ibid.* 80, 177 (1966); N. K. Glendenning and M. Veneroni, Phys. Rev. 144, 839 (1966).

[2]S. M. Austin, P. J. Locard, W. Benenson, and G. M. Crawley, Phys. Rev. 176, 1227 (1968).

[3]P. J. Locard, S. M. Austin, and W. Benenson, Phys. Rev. Letters 19, 1141 (1967).

[4]J. D. Anderson, S. D. Bloom, C. Wong, W. F. Hornyak, and V. A. Madsen, Phys. Rev. 177, 1416 (1969).

[5]G. C. Ball and J. Cerny, Phys. Rev. 177, 1466 (1969).

[6]A. S. Clough, C. J. Batty, B. E. Bonner, C. Tschälar, L. E. Williams, and E. Friedman, Nucl. Phys. A137, 222 (1969).

[7]J. D. Anderson, C. Wong, and V. A. Madsen, private communication.

[8]G. R. Satchler, Nucl. Phys. A95, 1 (1967).

[9]R. Reif, J. Slotta, and J. Höhn, Phys. Letters 26B, 484 (1968); and private communication.

[10]A. Scott, N. P. Mathur, and G. R. Satchler, to be published.

[11]Y. Awaya, J. Phys. Soc. Japan 23, 673 (1967).

[12]W. Benenson, S. M. Austin, R. A. Paddock, and W. G. Love, Phys. Rev. 176, 1268 (1968).

[13]A. Scott, M. L. Whiten, and W. G. Love, Nucl. Phys. A137, 445 (1969).

[14]V. Gillet and N. Vinh Mau, Nucl. Phys. 54, 321 (1964).

[15]H. Appel, S. N. Bunker, J. M. Cameron, M. B. Epstein, J. R. Quinn, J. R. Richardson, and J. W. Verba, Bull. Am. Phys. Soc. 13, 680 (1968); S. N. Bunker, H. Appel, J. M. Cameron, M. B. Epstein, J. R. Quinn, J. R. Richardson, and J. W. Verba, Bull. Am. Phys. Soc. 14, 529 (1969); S. N. Bunker, Ph.D. thesis, University of California, Los Angeles, California, 1970 (unpublished.

[16]The strongest indication of the possibility of multiple-excitation processes is the excitation of the 8.88-MeV state by inelastic α scattering; see, for example, W. W. Eidson and J. G. Cramer, Jr., Phys. Rev. Letters 9, 497 (1962).

[17]J. M. Cameron, J. R. Richardson, W. T. H. van Oers, and J. W. Verba, Phys. Rev. 167, 908 (1968).

[18]Kapton H film made by E. I. DuPont de Nemours, Wilmington, Delaware.

[19]T. Lauritsen and F. Ajzenberg-Selove, in *Nuclear Data Sheets*, compiled by K. Way *et al.* (Printing and Publishing Office, National Academy of Sciences – National Research Council, Washington, D. C., 1962), Sets 5 and 6; C. P. Browne and I. Michael, Phys. Rev. 134, B133 (1964); J. D. Larson and T. A. Tombrello, Phys. Rev. 147, 760 (1966).

[20]W. F. Hornyak and R. Sherr, Phys. Rev. 100, 1409 (1955).

[21]L. H. Johnston, D. H. Service, and D. A. Swenson, IRE Trans. Nucl. Sci. NS5, 95 (1958); D. F. Measday, Nucl. Instr. Methods 34, 353 (1965); D. F. Measday and C. Richard-Serre, *ibid.* 76, 45 (1969); J. N. Palmieri and J. Wolfe, *ibid.* 76, 55 (1969).

[22]E. A. Silverstein, Nucl. Instr. Methods 4, 53 (1959).

[23]B. M. Bardin and M. E. Rickey, Rev. Sci. Instr. 35, 902 (1964); R. Smythe, *ibid.* 35, 1197 (1964).

[24]W. W. Daehnick, Phys. Rev. 135, B1168 (1964).

[25]G. M. Crawley and G. T. Garvey, Phys. Rev. 160,

981 (1967).
[26]D. C. Larson and D. Bayer, private communication.
[27]D. J. Rowe, A. B. Clegg, G. L. Salmon, and P. S. Fisher, Proc. Phys. Soc. (London) 80, 1205 (1962).
[28]W. Benenson and G. M. Crawley, Bull. Am. Phys. Soc. 11, 477 (1966).
[29]H. B. Eldridge, S. N. Bunker, J. M. Cameron, J. R. Richardson, and W. T. H. van Oers, Phys. Rev. 167, 915 (1969); E. T. Boschitz, M. Chabre, H. E. Conzett, and R. J. Slobodrian, in *Proceedings of the Second International Symposium on the Polarization Phenomena of Nucleons, Karlsruhe, 1965,* edited by P. Huber and H. Schopper (Birkhäuser Verlag, Stuttgart, Germany, 1966), p. 331.
[30]W. T. H. van Oers and J. M. Cameron, Phys. Rev. 184, 1061 (1969).
[31]G. R. Satchler, Nucl. Phys. A100, 497 (1967).
[32]J. L. Snelgrove and E. Kashy, Phys. Rev. 187, 1246 (1969).
[33]F. Petrovich, H. McManus, V. A. Madsen, and J. Atkinson, Phys. Rev. Letters 22, 895 (1969).
[34]F. Petrovich, D. Slanina, and H. McManus, Michigan State University Report No. MSPT-103, 1967 (unpublished).
[35]F. Petrovich, Ph.D. thesis, Michigan State University, 1970 (unpublished).
[36]F. Petrovich, H. McManus, and J. R. Borysowicz, to be published.
[37]L. R. B. Elton, *Nuclear Sizes* (Oxford University Press, New York, 1961).
[38]This code was written by R. Haybron and T. Tamura and was modified for the Sigma 7 computer by J. J. Kolata.
[39]G. M. Crawley, private communication.
[40]F. A. Schmittroth, Ph.D. thesis, Oregon State University, 1969 (unpublished).
[41]J. C. Bergstrom, W. Bertozzi, S. Kowalski, X. K. Maruyama, J. W. Lightbody, Jr., S. P. Fivozinsky, and S. Penner, Phys. Rev. Letters 24, 152 (1970).
[42]V. Gillet and M. A. Melkanoff, Phys. Rev. 133, B1190 (1964).
[43]F. Petrovich, private communication.
[44]T. Hamada and I. D. Johnston, Nucl. Phys. 34, 382 (1962).
[45]J. Atkinson and V. A. Madsen, Phys. Rev. C 1, 1377 (1970).
[46]J. S. Blair, N. Cue, and D. Shreve, University of Washington Annual Report, 1965 (unpublished).
[47]H. McManus, private communication.
[48]M. Reed, Ph.D. thesis, University of California, Berkeley, Report No. UCRL-18414, 1968 (unpublished).
[49]A. Galonsky, private communication.
[50]F. Ajzenberg-Selove and T. Lauritsen, Nucl. Phys. 11, 1 (1959).

PHYSICAL REVIEW C VOLUME 3, NUMBER 4 APRIL 1971

Effective-Interaction Theory of Nuclear Spectral Relations. II*

Philip Goode, Daniel S. Koltun†, and Bruce J. West
Department of Physics and Astronomy, University of Rochester, Rochester, New York 14627
(Received 3 December 1970)

A theory of particle-hole relations among spectra, presented in Part I, is extended to include hole-hole (hh) spectra as well as the particle-particle (pp) and particle-hole (ph) cases previously treated. This theory, which incorporates configuration mixing into many-body effective interactions, goes beyond the simple shell-model particle-hole relations of Pandya, Goldstein, and Talmi. A new shell-model relation involving all three partners (the triptych: pp, ph, and hh) is derived. We apply the many-body theory and the triptych relation to the nuclei ^{42}Sc, ^{48}Sc, and ^{54}Co, which are partners in the $f_{7/2}$ shell. We find that we can then relate the spectra of these three nuclei to considerably greater accuracy than do the standard shell-model relations.

1. INTRODUCTION

In a previous paper[1] (which we will refer to as I) we developed the theoretical relationship between the energy spectra of two nuclei whose simple j-j coupling shell-model descriptions are *particle-particle*, with orbits (j, k), and *particle-hole*, with orbits (j, k^{-1}). In this paper we extend our considerations to include the *hole-hole* nucleus with orbits (j^{-1}, k^{-1}). In I we applied our theory to the model $f_{7/2}$-shell spectra of ^{42}Sc and ^{48}Sc. In the present work we shall report results for their hole-hole partner, ^{54}Co, and some further results for the two Sc isotopes.

In I we used the *effective-interaction* formulation of the many-body spectroscopic problem, in which the model states remain simple, and all effects of configuration mixing into the model states are included in the effective interaction. This interaction is then expressed as a perturbation expansion in terms of the free nucleon-nucleon interaction, as in Brueckner-Goldstone theory. In the present paper, we calculate the effects of configuration mixing by using shell-model matrix methods as an extension of the perturbation calculations in I. The application of matrix methods in